THE JOURNAL OF PHYSICAL CHEMISTRY B

ARTICLE

pubs.acs.org/JPCB

Development of an Optimized Intermolecular Potential for Sulfur Dioxide

MaryBeth H. Ketko,[†] Ganesh Kamath,[‡] and Jeffrey J. Potoff*[,†]

[†]Department of Chemical Engineering and Materials Science, Wayne State University, Detroit, Michigan 48202, United States

[‡]Computer Science and Mathematics Division, Oak Ridge National Laboratory, Oak Ridge, Tennessee 37830, United States

Supporting Information

ABSTRACT: A new force field for sulfur dioxide, capable of predicting accurately the vapor−liquid equilibria, critical properties, vapor pressure, and heats of vaporization is presented. The new force field reproduces the saturated liquid densities, vapor pressures and heats of vaporization to within 0.5, 2, and 2% of experiment, respectively. The predicted critical properties and the normal boiling point are in excellent agreement with experimental results. Pair distribution functions are calculated for the S−S, S−O, and O−O interactions are in close agreement with neutron and X-ray scattering experiments. In addition to the new force field, similar calculations are performed for four SO_2 intermolecular potentials proposed by Sokolic et al. (Sokolic, F.; Guissani, Y.; Guillot, B. J. Phys. Chem. 1985, 89, 3023], which show that these models work reasonably well near the state point where they were originally parametrized, but large errors in the predicted coexistence properties are displayed at higher and lower temperatures. Comparison of the radial distribution functions show the local structure is only weakly affected by the different force field parameters.

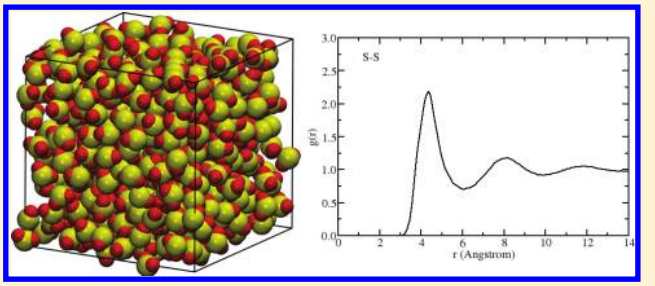

1. INTRODUCTION

Sulfur dioxide (SO_2) is a colorless, nonflammable gas with a pungent odor and is widely used as food preservative for dried fruits and in wine making. Prior to 1940, SO_2 was a common working fluid in refrigeration systems[1] but fell into disuse over concerns of toxicity after the development of fluorocarbon-based refrigerants, such as Freon (R-12). SO_2 is also a byproduct of coal combustion and reacts with water to form sulfuric acid (acid rain).

Recently, experiments have shown ionic liquids (IL) to be promising materials for the physical adsorption of SO_2 from flue gas.[2−6] However, given the extraordinary number of potential ionic liquids, determination of the optimal combination of anion and cation from trial and error is likely to be an arduous process. Computational methods, such as Monte Carlo and molecular dynamics simulations, hold promise for prescreening candidate ionic liquids for SO_2-philicity as well as providing fundamental information on molecular level interactions that could be exploited to develop optimal IL for SO_2 capture.

Indeed, molecular dynamics simulations have been used to study the behavior of SO_2 at the air/water[7] and air/IL interface[8] and the effect of SO_2 on the structure and dynamics of 1-butyl-3-methylimidazolium bromide.[9] However, the reliability to the SO_2 models used in these studies and others[10] is not clear. Ribeiro used molecular dynamics simulations to show that the Sokolic model for SO_2 produced low temperature molar volumes and liquid structures in close agreement with experimental values.[11] Gibbs ensemble Monte Carlo simulations of this force field also predicted saturated liquid densities in close agreement with experiment over a narrow range of temperatures, but vapor pressures were under-predicted by 20−50%.[12] In addition to the standard 12-6 Lennard-Jones plus point charge style models, more complex force fields for SO_2 have been proposed that include polarizability,[7] use point dipoles and quadrupoles instead of point charges,[13] or use 9-6 Lennard-Jones potentials.[14] Of these force fields, only the work of Eckl et al. was optimized for the accurate prediction of vapor−liquid equilibria[13]

In this work, we present an optimized force field for SO_2, derived from the Transferable Potentials for Phase Equilibria (TraPPE) parameter set, which is capable of reproducing saturated liquid densities, vapor pressures, and heats of vaporization to within 0.5, 2, and 2% of experiment, respectively. This force field uses a standard Lennard-Jones 12-6 potential and point charges and therefore is compatible with all popular simulation engines. In addition, the liquid−vapor coexistence curves, vapor pressures, and heats of vaporization are calculated for four parameter sets published by Sokolic et al.[15] For all models, grand canonical histogram reweighting Monte Carlo simulations are used to determine the vapor−liquid coexistence curves, vapor pressures, and heats of vaporization. Liquid phase structures are determined from isobaric−isothermal (NPT) simulations and

Received: February 1, 2011
Revised: March 23, 2011
Published: April 08, 2011

Table 1. Non-Bonded Parameters for Various SO_2 Force Fields

force field	site	ε/k_b (K)	σ (Å)	q_i (e)
this work	O	79.0	3.05	−0.295
	S	73.8	3.39	+0.59
Sokolic A	O	63.2	2.988	−0.234
	S	155.5	3.575	+0.468
Sokolic B	O	62.3	2.993	−0.234
	S	154.5	3.585	+0.468
Sokolic C	O	58.6	2.998	−0.234
	S	148.0	3.605	+0.468
Sokolic D	O	57.5	3.005	−0.234
	S	146.0	3.615	+0.468

compared to experimental neutron and X-ray scattering data. Self-diffusion coefficients are computed for each force field using molecular dynamics simulations in the microcanonical ensemble.

2. FORCE FIELD

All interaction sites for dispersive and electrostatic interactions are placed on the nuclei of the sulfur and oxygen atoms. Nonbonded interactions are described by a pairwise-additive Lennard-Jones (12-6) plus point charge functional form

$$U(r_{ij}) = 4\varepsilon_{ij}\left[\left(\frac{\sigma_{ij}}{r_{ij}}\right)^{12} - \left(\frac{\sigma_{ij}}{r_{ij}}\right)^{6}\right] + \frac{q_i q_j}{4\pi\varepsilon_0 r_{ij}} \quad (1)$$

where r_{ij}, ε_{ij}, σ_{ij}, q_i, and q_j are the separation, LJ well depth, LJ size, and partial charges, respectively, for the pair of interaction sites i and j. ε_0 is the permittivity of vacuum. The optimized potential parameters for sulfur dioxide, as well as the parameters for the Sokolic[15] force fields, are listed in Table 1. Interactions between unlike atoms are computed with the Lorentz−Berthelot combining rules[16]

$$\sigma_{ij} = \frac{\sigma_{ii} + \sigma_{jj}}{2} \quad (2)$$

$$\varepsilon_{ij} = \sqrt{\varepsilon_{ii}\varepsilon_{jj}} \quad (3)$$

Oxygen and sulfur atoms were connected by rigid bonds with length 1.432 Å.[18] A harmonic potential was use to govern bond angle bending

$$U_{\text{bend}} = \frac{k_\theta}{2}(\theta - \theta_o)^2 \quad (4)$$

where $\theta_o = 119.3°$ is the equilibrium bond angle and $k_\theta = 55{,}357$ K/rad^2. Both values were determined from MP2/6-31+g(d,p) ab initio calculations performed with Gaussian 03.[17]

3. SIMULATION DETAILS

Vapor−liquid coexistence curves, vapor pressures, and heats of vaporization were calculated from histogram reweighting Monte Carlo simulations in the grand canonical ensemble.[19,20] The ratios of attempted moves for each simulation were 60% particle insertions/deletions, 20% translations, and 20% rigid rotations. Configurational-bias methods were used to enhance the acceptance rate for molecule insertions.[21] A box length of

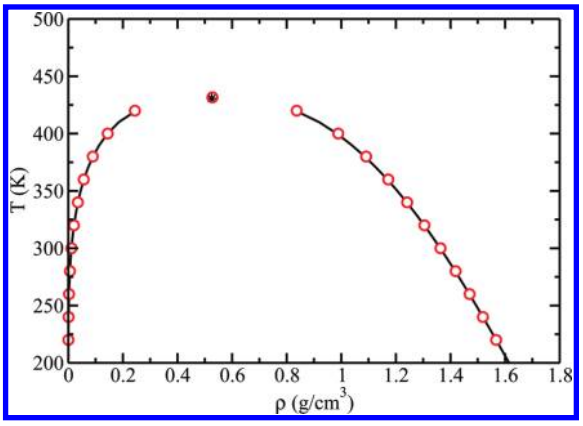

Figure 1. Vapor−liquid coexistence curve for SO_2 predicted by the new force field. Simulation data are shown as circles, while the solid line represents data from NIST chemistry webbook.[42]

L = 25 Å was used for all calculations. Additional calculations were performed for L = 30 Å to verify the predicted results were invariant with system size. Lennard-Jones interactions were truncated at 10 Å and analytical tail corrections were applied.[16] An Ewald sum with tinfoil boundary conditions was used for the calculation of electrostatic interactions.[16]

A total of 10 Monte Carlo simulations were required to construct the entire vapor−liquid coexistence curve from 230−430 K: 1 simulation bridging liquid and vapor phases near the critical point, 2 vapor phase simulations at 420 and 380 K, and 7 liquid phase simulations performed at 410, 380, 350, 320, 290, 260, and 230 K. Each simulation was performed for 20 million Monte Carlo steps (MCS). The first one million Monte Carlo steps of each simulation were used as an equilibration and the data resulting from these time periods were discarded. Statistical uncertainties were estimated as the standard deviation of three unique sets of simulation data, each started from different initial configurations and random number seeds.

Radial distribution functions were extracted from NPT molecular dynamics simulations, which were performed using NAMD version 2.7.[22] Simulations were performed for 10 ns with a 2 fs time step. Nonbonded pair lists were maintained at 16 Å with a Lennard-Jones cutoff at 14 Å . The particle-mesh Ewald (PME) was used to calculate long-range electrostatic interactions. All simulations were performed on cubic boxes containing 500 SO_2 molecules. Diffusion coefficients were determined from simulations in the microcanonical ensemble (NVE). Three sets of 0.5 ns simulations, using a 1 fs time step, were performed to gather statistics at four different temperatures (220, 258, 300, and 340 K). Calculations at all temperatures were performed at densities predicted from NPT simulations at 258 K and 1.01 bar. The temperature for each set of NVE simulations was set using a 1 ns simulation in the canonical ensemble.

4. RESULTS AND DISCUSSION

In Figure 1, the vapor−liquid coexistence behavior predicted by our optimized force field for SO_2 is presented. The maximum deviation between simulation and experiment is 0.5%, which is within the statistical uncertainty of the calculation. Parameters were optimized following the methodology outlined in our previous work for H_2S[23] and dimethyl ether.[24] Initial estimates of Lennard-Jones parameters for sulfur and oxygen were taken

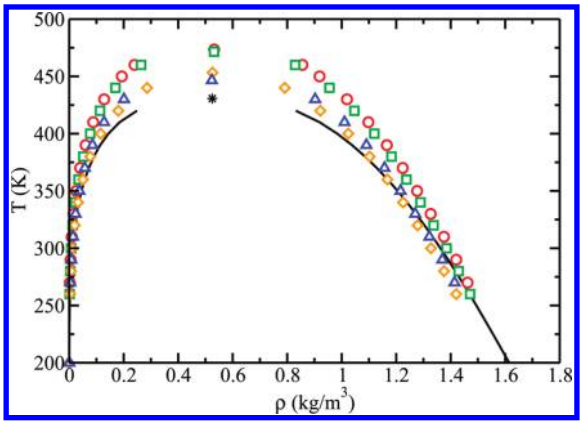

Figure 2. Vapor−liquid coexistence curve for SO_2 predicted by various force fields propsed by Sokolic et al.[15] Model A (circles), Model B (squares), Model C (diamonds), and Model D (triangles). Solid line represents data from NIST chemistry webbook.[42]

from the TraPPE; sulfur parameters were taken from dimethyl sulfide[25] and oxygen parameters from carbon dioxide.[26] In an effort to minimize the number of free parameters, only Lennard-Jones parameters for the sulfur atom and the partial charge distribution (note: $q_S = 2|q_O|$) were altered during the optimization process. The choice to optimize Lennard-Jones parameters for the sulfur atom only was based on the new bonding environment for sulfur. Initial parameters for sulfur were taken from dimethylsulfide, where sulfur exists in the sp^3 hybridization state. However, in SO_2, sulfur is sp^2 hybridized, requiring a reoptimization of Lennard-Jones parameters. Oxygen parameters, taken from CO_2, already correspond sp^2 hybridization and have been used successfully in other force fields for aldehydes,[27] ketones,[27] carboxylic acids[28] and phosphate esters.[29]

Usually initial estimates of partial charges are determined from a CHELPG analysis of electrostatic potential energy surfaces generated from HF/6-31+g(d,p) calculations. However, in this case, unusually large partial charges were predicted ($q_S = 0.734$); all attempts to optimize Lennard-Jones parameters for the sulfur atom failed. Instead, a series of optimized Lennard-Jones parameters were determined for various partial charge distributions $0.52 < q_S < 0.68$. As in prior work, it was possible to match experimental saturated liquid densities for nearly all partial charge distributions.[24] However, the vapor pressure was a strong function of partial charge, and the parameters listed in Table 1 correspond to the best overall fit to the experimental data.

Vapor−liquid coexistence curves predicted by four parameter sets (models A, B, C, and D) proposed by Sokolic et al.[15] are presented in Figure 2. These models were developed by fitting each one to saturated liquid densities at a specific temperature along the coexistence curve: 220, 250, 323.16, and 350 K for models A, B, C and D, respectively. For all models, partial charges of $q_S = 0.468$, $q_O = -0.234$ were selected to reproduce the gas phase dipole moment $\mu = 1.62$ D. The various parameter sets do a good job reproducing the saturated liquid density at the temperature for which they were parametrized. However, at temperatures above and below the state point where the models were fit, deviations of ±5−10% from experimental data were observed. The overprediction of saturated liquid densities above the optimization temperature, and under-prediction of saturated liquid densities below it suggests two flaws: the ratio of σ_S/σ_O is too large, and the overall attractive force between atoms is too large.

Table 2. Predicted Critical Parameters and Normal Boiling Points[a]

model	T_c (K)	ρ_c (g/cm^3)	P_c (bar)	T_b (K)
experiment[33,34,41]	430.8	0.525	78.831	263
this work	431.6(3)	0.528(2)	79.2(2)	263.0(7)
Sokolic A	473.5(4)	0.532(2)	93.6(3)	274.7(2)
Sokolic B	471.5(1)	0.532(3)	94.6(5)	272.5(6)
Sokolic C	453.3(3)	0.526(1)	90.1(1)	263.0(7)
Sokolic D	446.6(2)	0.523(1)	87.1(3)	259.6(9)

[a] Numbers in parentheses represent the uncertainty in the last digit.

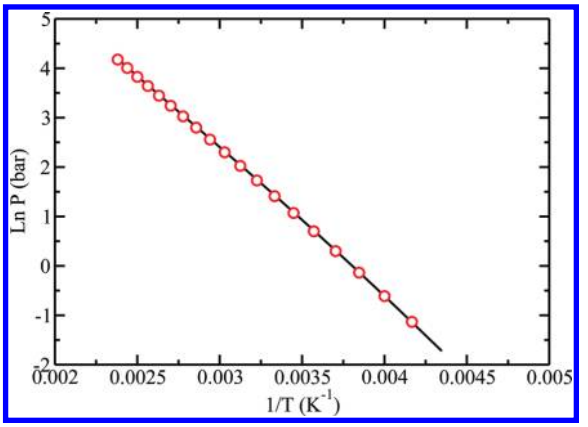

Figure 3. Vapor pressure as a function of temperature for SO_2 predicted by the new force field. Simulation data are shown as circles, while the solid line represents data from NIST chemistry webbook.[42]

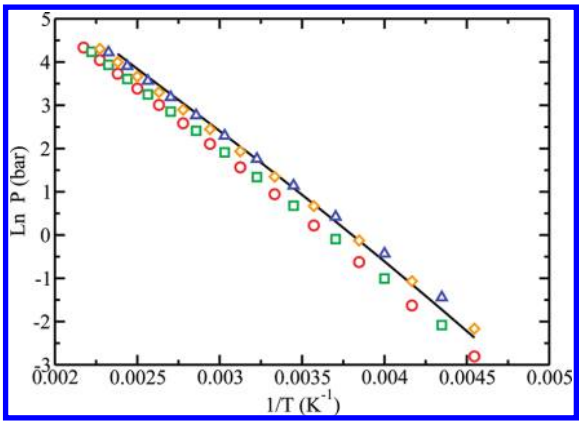

Figure 4. Vapor pressure as a function of temperature for SO_2 predicted by various force fields propsed by Sokolic et al.[15] Model A (circles), Model B (squares), Model C (diamonds), and Model D (triangles). Solid line represents data from NIST chemistry webbook.[42]

Critical parameters were determined for all models by fitting the saturated liquid and vapor densities to the density scaling law for critical temperature[30]

$$\rho_{liq} - \rho_{vap} = B(T - T_c)^{\beta} \quad (5)$$

and the law of rectilinear diameters[31]

$$\frac{\rho_{liq} + \rho_{vap}}{2} = \rho_c + A(T - T_c) \quad (6)$$

dx.doi.org/10.1021/jp2010524 |J. Phys. Chem. B 2011, 115, 4949–4954

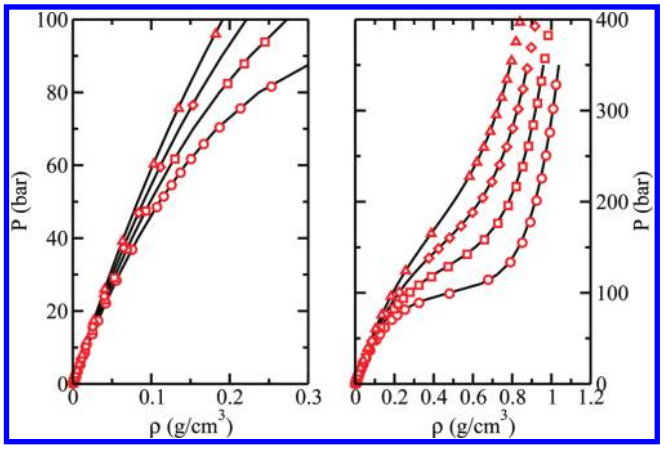

Figure 5. Pressure−density isotherms for SO_2 predicted by the new force field at 448.15 K (circles), 473.15 K (squares), 498.15 K (diamonds), and 525.0 K (triangles). Solid line represents data from NIST chemistry webbook.[42]

where $\beta = 0.325$ is the critical exponent for Ising-type fluids in three dimensions.[32] Predicted critical parameters for each force field are listed in Table 2. The new force field predicts the T_c = 431.6 K, which is within 1 K of the experimental value. The predicted critical pressure of P_c = 79.2 bar is within 0.4 bar of the experimental value of 78.831.[33] Of the Sokolic force fields, model D gives the closest reproduction of the critical parameters, overpredicting the critical temperature and pressure by 4% and 11%, respectively.

In Figures 3 and 4, vapor pressures predicted by the new force field and the various Sokolic parameter sets are presented with experimental data for comparison. The new force field predicts vapor pressures within 2% of experiment for 230 K < T < 420 K. Interpolation of the vapor pressure data predicted by simulation yields a normal boiling point of 263.0 ± 0.7 K, which is identical to the experimental value.[34] Vapor pressures predicted by the Sokolic models display large errors compared to experimental data. Models A and B underpredict vapor pressures by 30−40%. The accentric factor ω predicted by Models C and D is too low, resulting in a crossing of the experimental vapor pressure data. As a result, for a narrow range of temperatures, 250−280 K for model C and 280−340 K for model D, vapor pressures are predicted to within ±5% of experimental data. Outside of these temperature ranges errors of ±10−20% were observed.

The vapor pressure provides important insight into interactions between molecules. While the saturated liquid densities and critical temperature are controlled by the overall magnitude of interactions and the size of the atoms, the vapor pressure is related to the range of interaction between molecules.[35] Since the range of interaction is largely determined by magnitude and distribution of partial charges,[24] the vapor pressure can be used for determining the correct balance of dispersive and electrostatic interactions. For force fields that provide similar reproduction of experimental saturated liquid densities, increasing the magnitude of the partial charges causes the acentric factor ω to increase.[23,24,36] On the basis of the results of these calculations, it is clear that the Sokolic models underestimate the Coloumbic contribution to the intermolecular potential. These data also suggest that the polarizable force field of Baer et al.,[7] which uses similar partial charges of q_S = 0.470, also underestimates Coulombic contributions.

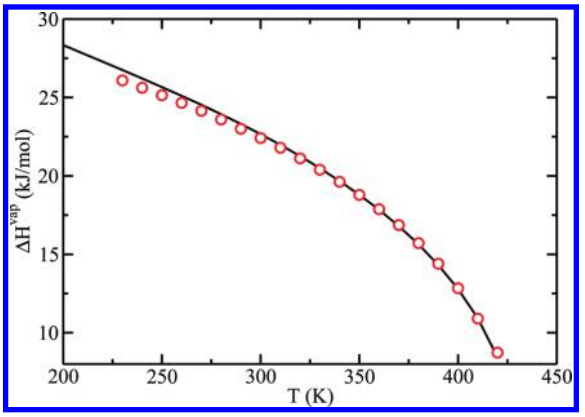

Figure 6. Heat of vaporization for SO_2 predicted by the new force field. Simulation data are shown as circles, while the solid line represents data from NIST chemistry webbook.[42]

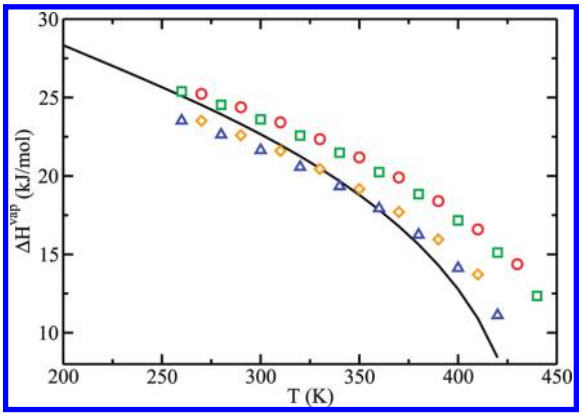

Figure 7. Heat of vaporization for SO_2 predicted by various force fields proposed by Sokolic et al.[15] Model A (circles), Model B (squares), Model C (diamonds), and Model D (triangles). Solid line represents data from NIST chemistry webbook.[42]

As a further test of the predictive capabilities of the new SO_2 force field, pressure−density isotherms were predicted in the supercritical phase for 448.15 K ≤ T ≤ 525 K and are shown in Figure 5. For all temperatures, the new force field provides an excellent reproduction of experimental data, illustrating the transferability of the proposed potential parameters to a wide range of temperatures and pressures.

The heat of vaporization ΔH_v was calculated over the temperature range 240 K ≤ T ≤ 420 K and is shown in Figure 6 for the new force field and Figure 7 for the Sokolic models. Since the enthalpy is defined as $H = U + pV$, ΔH_v can be calculated directly from

$$\Delta H_v = U_v - U_l + p \times (V_v - V_l) \quad (7)$$

where the v and l subscripts refer to the vapor and liquid phases, U is the internal energy per mol, and V is the molar volume. The energies and molar volumes of each phase were determined from the same histogram data collected for the VLE calculations. For the new force field, heats of vaporization are predicted to within 2% of experimental data, which is to be expected given the close agreement of the vapor pressure and saturated liquid densities with experimental data. The Sokolic models C and D exhibit relatively good agreement with experimental data between 250 and 380 K, while deviations of over 10% were observed at higher temperatures.

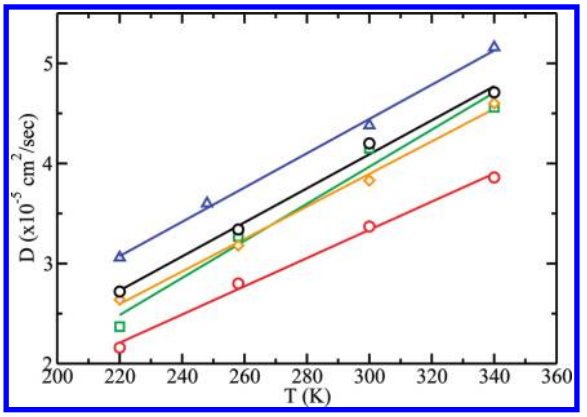

Figure 8. Self-diffusion coefficient for SO_2 predicted by various force fields for $220 \leq T \leq 340$ K. New (black circles), Model A (red circles), Model B (squares), Model C (diamonds), and Model D (triangles). Lines are linear regression fits to the data.

Calculation of the diffusion coefficient requires computation of mean square displacements (MSD) of the center of mass of the molecules. The MSD as a function of time were calculated using the PTRAJ facility in AMBER-10.[37] The slope of the MSD vs time provides an estimate of the self-diffusion coefficient[38]

$$D = \lim_{t \to \infty} \Sigma \frac{\langle [r_i(t) - r_i(0)]^2 \rangle}{6t} \quad (8)$$

In Figure 8, the self-diffusion coefficient for SO_2, predicted by the new model and the Sokolic models, at four different temperatures is presented. As expected, the diffusion coefficient increases linearly with increasing temperature for all SO_2 models. The diffusion coefficients are in fair agreement with the earlier predictions of the Sokolic models[15] and decrease with increasing interactions between molecules. The new force field, despite having the lowest overall interactions between molecules, predicts diffusion coefficients between Sokolic models C and D. This is due to a 20% increase in electrostatic interactions, which leads to slightly increased long-range order. Similar effects of increased long-range order on the lowering of self-diffusion coefficients has been observed for calculations performed with the SPC and TIP3P water models.[39]

The local microstructure of liquid phase SO_2 was determined from pair distribution functions extracted from NPT molecular dynamics simulations at 258 K and 1 bar, which corresponds the conditions of X-ray and neutron scattering experiments.[40] Figure 9 shows the three partial distribution functions contributing to the overall structure of liquid SO_2. The new model exhibits a sharper peak for the O−O RDF at 3.4 Å in comparison to the plateau predicted by the Sokolic models. Each model displays a strong intramolecular contribution at 3.4 Å, which agrees with previous neutron and X-ray studies.[40] The presence of the first solvation shell around 3.4 Å is also in agreement with earlier neutron scattering experiments, which place the O−O interactions in the 3.26−3.70 Å range.[40] Partial structure factors, derived from the neutron total structure factor, suggest a peak at 3.5 Å, which is in excellent agreement with O−O peak seen for the new model. The presence of a slightly more defined second solvation shell around 7 Å for the new model is likely the result of increased long-ranged electrostatic interactions.

Figure 9b shows the $g(r)$ for S−O interactions in SO_2. All the models show a weak hump around 3.4 Å and a shoulder around

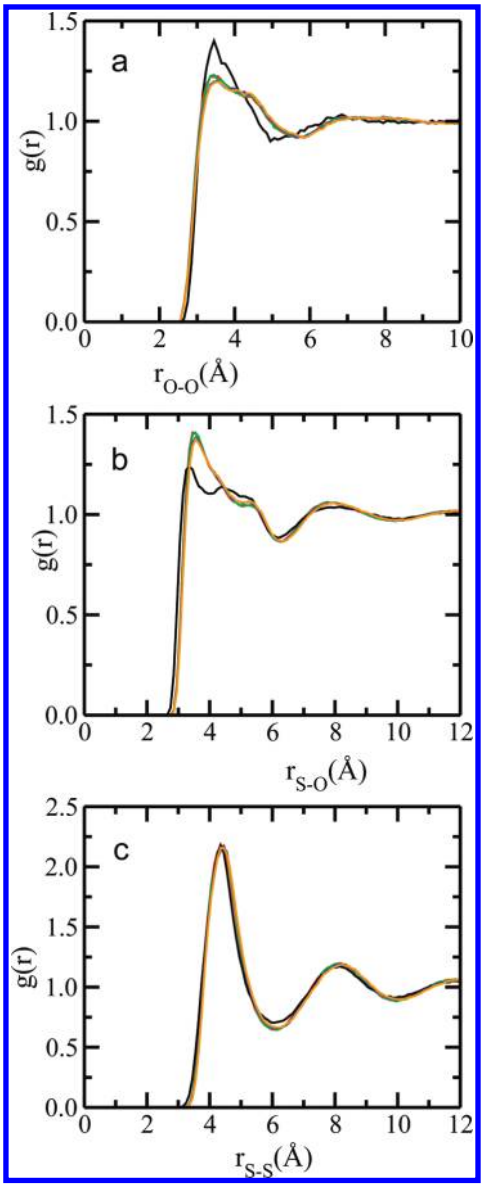

Figure 9. Radial distribution functions for SO_2 predicted by various force fields at 258 K and 1.01 bar. New (black), Model A (red), Model B (green), Model C (orange), Model D (blue).

5.5 Å, which is in good agreement with the neutron scattering data. The new model, however, exhibits a lower and broader peak height for the S−O interaction at 3.4 Å in comparison to the Sokolic models. In Figure 9c, the $g(r)$ for S−S interactions is presented. All the models show a strong peak at 4.35 Å which is in excellent agreement the 4.25 Å predicted by neutron and X-ray scattering experiments. While significant differences were observed for the $g(r)$ predicted by the new and Sokolic models for S−O and O−O interactions, the S−S $g(r)$ is largely unaffected by the choice of force field.

5. CONCLUSIONS

We have developed a three site, Lennard-Jones plus point charge model for sulfur dioxide that is capable of reproducing saturated liquid densities, vapor pressures, heats of vaporization, and critical properties to high accuracy. The force field presented

in this work provides improved predictions of saturated liquid densities and vapor pressures for $T \leq 300$ K compared to the Eckl force field,[13] but otherwise the models are of similar accuracy.

In addition, extensive calculations were performed on the SO_2 force fields proposed by Sokolic, some of which have been used in the simulation of SO_2 interactions with ionic liquids.[9] Our calculations show these force fields exhibit large deviations from experimental saturated liquid densities, vapor pressures, and heats of vaporization. The vapor pressure data suggest that these force fields significantly under-predict the Coulombic contribution to the intermolecular potential. Other force fields for SO_2 that utilize similar partial charges[7,8] are expected to exhibit similar problems. Because of the strong electrostatic interactions present in ionic liquids, inadequate representation of such interactions by the SO_2 force field may lead to significant errors in the predicted solubility and/or liquid phase microstructure. Quantifying these effects is the focus of ongoing work in our group.

■ ASSOCIATED CONTENT

Supporting Information. Predictions of various parameter sets optimized with different partial charges, and the Sokolic force fields using truncated Lennard-Jones potentials are presented. Furthermore, all data presented in this work have been tabulated. This material is available free of charge via the Internet at http://pubs.acs.org.

■ AUTHOR INFORMATION

Corresponding Author

*E-mail: jpotoff@wayne.edu. Fax: 313 578 5815. Phone: 313 577 9357.

■ ACKNOWLEDGMENT

Financial support from a Wayne State University Undergraduate Research and Creative Projects Grant (M.B.H.K.), NSF CBET-0730768 (J.J.P.) and ORISE/ORAU (G.K.) is gratefully acknowledged. The authors acknowledge CPU time provided by Grid Computing at Wayne State University.

■ REFERENCES

(1) Johnston, C. W. *Ind. Eng. Chem.* **1932**, *24*, 626.
(2) Wu, W.; Han, B.; Gao, H.; Liu, Z.; Huang, J. *Angew. Chem., Int. Ed.* **2004**, *43*, 2415.
(3) Anderson, J. L.; Dixon, J. K.; Maginn, E. J.; Brennecke, J. F. *J. Phys. Chem. B* **2006**, *110*, 15059.
(4) Huang, J.; Riisanger, A.; Wasswerscheid, P.; Fehrmann, R. *Chem. Commun.* **2006**, 4027.
(5) Jiang, Y.-Y.; Zhou, Z.; Jiao, Z.; Li, L.; Wu, Y.-T.; Zhang, Z.-B. *J. Phys. Chem. B* **2007**, *111*, 5058.
(6) Shiflett, M. B.; Yokozeki, A. *Energy Fuels* **2010**, *23*, 1001.
(7) Baer, M.; Mundy, C. J.; Chang, T.-M.; Tao, F.-M.; Dang, L. X. *J. Phys. Chem. B* **2010**, *114*, 7245.
(8) Wick, C.; Chang, T.-M.; Dang, L. X. *J. Phys. Chem. B* **2010**, *114*, 14965.
(9) Siqueira, L. J. A.; Ando, R. A.; Bazito, F. F. C.; Torresi, R. M.; Santos, P. S.; Ribeiro, M. C. C. *J. Phys. Chem. B* **2008**, *112*, 6430.
(10) Wang, Y.; Pan, H.; Li, H.; Wang, C. *J. Phys. Chem. B* **2007**, *111*, 10461.
(11) Ribeiro, M. C. C. *J. Phys. Chem. B* **2006**, *110*, 8789.
(12) Shi, W.; Maginn, E. J. *J. Comput. Chem.* **2008**, *29*, 2520.
(13) Eckl, B.; Vrabec, J.; Hasse, H. *J. Phys. Chem. B* **2008**, *112*, 12710.
(14) Yang, J.; Ren, Y.; Tian, A. *J. Phys. Chem. B* **2000**, *104*, 4951.
(15) Sokolic, F.; Guissani, Y.; Guillot, B. *J. Phys. Chem.* **1985**, *89*, 3023.
(16) Allen, M. P.; Tildesley, D. J. *Computer Simulation of Liquids*; Clarendon Press: Oxford, 1987.
(17) Frisch, M. J.; Trucks, G. W.; Schlegel, H. B.; Scuseria, G. E.; Robb, M. A.; Cheeseman, J. R.; Montgomery, J. A., Jr.; Vreven, T.; Kudin, K. N.; Burant, J. C.; Millam, J. M.; Iyengar, S. S.; Tomasi, J.; Barone, V.; Mennucci, B.; Cossi, M.; Scalmani, G.; Rega, N.; Petersson, G. A.; Nakatsuji, H.; Hada, M.; Ehara, M.; Toyota, K.; Fukuda, R.; Hasegawa, J.; Ishida, M.; Nakajima, T.; Honda, Y.; Kitao, O.; Nakai, H.; Klene, M.; Li, X.; Knox, J. E.; Hratchian, H. P.; Cross, J. B.; Bakken, V.; Adamo, C.; Jaramillo, J.; Gomperts, R.; Stratmann, R. E.; Yazyev, O.; Austin, A. J.; Cammi, R.; Pomelli, C.; Ochterski, J. W.; Ayala, P. Y.; Morokuma, K.; Voth, G. A.; Salvador, P.; Dannenberg, J. J.; Zakrzewski, V. G.; Dapprich, S.; Daniels, A. D.; Strain, M. C.; Farkas, O.; Malick, D. K.; Rabuck, A. D.; Raghavachari, K.; Foresman, J. B.; Ortiz, J. V.; Cui, Q.; Baboul, A. G.; Clifford, S.; Cioslowski, J.; Stefanov, B. B.; Liu, G.; Liashenko, A.; Piskorz, P.; Komaromi, I.; Martin, R. L.; Fox, D. J.; Keith, T.; Al-Laham, M. A.; Peng, C. Y.; Nanayakkara, A.; Challacombe, M.; Gill, P. M. W.; Johnson, B.; Chen, W.; Wong, M. W.; Gonzalez, C.; Pople, J. A. *Gaussian 03*, revision A.1; Gaussian, Inc.: Pittsburgh, PA, 2003.
(18) Pauling, L. *The Nature of the Chemical Bond*, 3rd ed.; Cornell University: Ithaca, 1960; p 328.
(19) Potoff, J. J.; Panagiotopoulos, A. Z. *J. Chem. Phys. 108*, 10914.
(20) Potoff, J. J.; Errington, J. R.; Panagiotopoulos, A. Z. *Mol. Phys.* **1999**, *97*, 1073.
(21) Martin, M. G.; Siepmann, J. I. *J. Phys. Chem. B* **1999**, *103*, 4508.
(22) Phillips, J. C.; Braun, R.; Wang, W.; Gumbart, J.; Tajkhorshid, E.; Villa, E.; Chipot, C.; Skeel, R. D.; Kale, L.; Schulten, K. *J. Comput. Chem.* **2005**, *26*, 1781.
(23) Kamath, G.; Lubna, N.; Potoff, J. J. *J. Chem. Phys.* **2005**, *123*, 124505.
(24) Ketko, M. B. H.; Potoff, J. J. *Mol. Sim.* **2007**, *33*, 769.
(25) Lubna, N.; Kamath, G.; Potoff, J. J.; Rai, N.; Siepmann, J. I. *J. Phys. Chem. B* **2005**, *109*, 24100.
(26) Potoff, J. J.; Siepmann, J. I. *AIChE J.* **2001**, *47*, 1676.
(27) Stubbs, J. M.; Potoff, J. J.; Siepmann, J. I. *J. Phys. Chem. B* **2004**, *108*, 17596.
(28) Kamath, G.; Cao, F.; Potoff, J. J. *J. Phys. Chem. B* **2004**, *108*, 14130.
(29) Sokkalingam, N.; Kamath, G.; Coscione, M.; Potoff, J. J. *J. Phys. Chem. B* **2009**, *113*, 14725.
(30) Rowlinson, J. S.; Widom, B. *Molecular Theory of Capillarity*; Clarendon Press: Oxford, 1982.
(31) Rowlinson, J. S.; Swinton, F. L. *Liquids and Liquid Mixtures*, 3rd ed.; Butterworth: London, 1982.
(32) Privman, V. In *Encyclopedia of Applied Physics*; Trigg, G. L., Ed.; Wiley-VCH: Berlin, 1998; Vol. 23, p 41.
(33) Valtz, A.; Coquelet, C.; Richon, D. *Fluid Phase Equilib.* **2004**, *220*, 77.
(34) Bergstrom, F. W. *J. Phys. Chem.* **1922**, *26*, 876.
(35) Potoff, J. J.; Bernard-Brunel, D. A. *J. Phys. Chem. B* **2009**, *113*, 10292.
(36) Peguin, R. P. S.; Kamath, G.; Potoff, J. J.; da Rocha, S. R. P. *J. Phys. Chem. B* **2008**, *113*, 178.
(37) Case, D. A.; Cheatham, T. E.; Darden, T.; Gohlke, H.; Luo, R.; Merz, K. M.; Onufriev, A.; Simmerling, C.; Wang, B.; Woods, R. J. *J. Comput. Chem.* **2005**, *26*, 1668.
(38) Haile, J. M. *Molecular Dynamics Simulation*; John Wiley & Sons Inc.: New York, 1997.
(39) Mark, P.; Nilsson, L. *J. Phys. Chem. A* **2001**, *105*, 9954.
(40) Yamaguchi, T.; Lindquist, O.; Dahlborg, U. *Acta Chem. Scand.* **1984**, *38*, 757.
(41) Kang, T. L.; Hirth, L. J.; Kobe, K. A.; McKetta, J. J. *J. Chem. Eng. Data* **1961**, *6*, 220.
(42) Lemmon, E. W.; McLinden, M. O.; Friend, D. G. Thermophysical Properties of Fluid Systems. In *NIST Chemistry WebBook, NIST Standard Reference Database Number 69*; Linstrom, P. J., Mallard, W. G., Eds.; National Institute of Standards and Technology: Gaithersburg, MD, 2005; p 20899 (http://webbook.nist.gov).